

Project: DOE-Las Vegas # DE-FG08-94NV11627

AISb Photonic Detectors for Gamma-Ray Spectroscopy

Progress Report for Period: Oct. 1994 to August 1995

Authors: P. Becla and A. F. Witt, MIT Cambridge, Ma 02139

RECEIVED
JAN 30 1996
OSTI**SUMMARY**

Aluminum antimony (AISb) is an indirect band gap semiconductor with Eg of about 1.62 eV at 300K and about 1.75 eV at 77K [1 to 5]. This material, is extremely difficult to obtain in single crystal form because of the very high reactivity of aluminum with oxygen, and the high volatility of antimony. Moreover, molten AISb reacts with nearly all crucible materials available. Since Welker's first attempts in 1952 [6,7], only very few different experimental approaches have been used to grow single crystals of AISb, e.g. by Bridgman [8,9],, Czochralski [10,12] and MBE [13]. All experimental results, however, indicate that many of the properties of AISb, e.g. carrier concentration, electron-hole mobility and carrier life-time, differ significantly from the theoretically predicted values.

The main objective of this research period has been to develop a method leading to improved crystallographic and electronic quality of AISb crystals, making them more suitable for device applications. The research program was aimed along the following two directions:

- (1) study the growth of AISb via Bridgman, Czochralski and THM techniques;
- (2) comprehensive characterization of grown material, related to the use of compounds for high energy gamma detectors.

Variables in the growth study were growth temperature, equilibrium pressure, growth rate, doping, crucible material, seeding and encapsulation. The characterization study included crystallographic quality (grain size, etch pits, precipitates, inclusions), electronic quality (conductivity type, carrier concentration and mobility), optical properties (spectral absorption, photoconductivity, persistent absorption) and others (SIMS, EPR).

1 BACKGROUND

AISb crystallizes in the sphalerite type lattice [14] with a lattice constant, a, in the range 6.136 Å [15] to 6.0959 Å [16]. The melting point is in the range 1052 °C [18] to 1080 °C [17], and the band gap is indirect [1]. The energy band structure of AISb is presented in fig.1. The first and second conduction band minima are located around the X Brillouin zone; the distance between the two conduction bands X₁ and X₃ is approximately 0.36 eV; between the conduction band X₁ and valence the band approximately 1.62 eV. The valence band

MASTER

consists of three subbands: the heavy and light hole bands and spin-orbit split band. The distance between the spin-orbit split band and the heavy and light hole bands is approximately 0.75 eV. The calculated mobilities of electrons and holes at 300 K are in the range $1100 \text{ cm}^2/\text{Vs}$ and $700 \text{ cm}^2/\text{Vs}$, respectively [3]. AlSb can be useful for electronic devices such as transistors and diodes at high temperatures [2] and is very promising for applications such as high energy photon detectors [3]. The photon dispersion curve [4,5] indicates positive dispersion in contrast to most of the other III-V compounds.

As-grown single crystals have been reported to always be p-type. It has been assumed that p-type conductivity was mainly due to the presence of residual acceptor impurities in the starting material. Blunt et al. [16] suggest that the cause of p-type conductivity could also be due to Sb vacancies; this suggestion agrees with Van Vechten's [19] findings, that the cause of p-type conductivity in AlSb is the lower tetratrahedral covalence radii (r_t) of one of the relevant elements, e.g. Al. The vacancy model also agrees with this event and suggests that the unpaired bonds of aluminum atoms are the cause of atmospheric deterioration of AlSb crystals [20]. The formation of intrinsic vacancies, V_{Al} and V_{Sb} , versus temperature was investigated by Sherohman [21]. According to the vacancy concentration diagram (see fig.2), at the highest temperature of the solid, 1052°C ($x_{\text{Sb}} = 0.499954$), there are $2.5 \times 10^{18} \text{ cm}^{-3}$ and $5.6 \times 10^{18} \text{ cm}^{-3}$ Al and Sb vacancies in the crystal. At the stoichiometric composition, $x_{\text{Sb}} = 0.5$, the vacancy concentration curves intersect at approximately 1040°C at which $V_{\text{Al}} = V_{\text{Sb}} = 3.15 \times 10^{18} \text{ vacancies/cm}^3$. Along the Al-rich liquidus, V_{Sb} does not change significantly with a decrease in temperature, which it does along the Sb-rich liquidus. For example, V_{Sb} is reduced by a factor of 5 at 1000°C and by a factor of 16 at 900°C .

The suitability of various crucible materials has studied:BN, Ta, MgO and Al_2O_3 . It has been shown that except for dense Al_2O_3 all crucible materials either react with the melt or cause excessive doping. Also, Mg, Cu, Fe, Si and C have been shown to produce p-type material. Attempts have been made to obtain n-type material in doping studies using Te and Se [22]; however, results indicate that n-type material can be obtained only after melt doping with significant amounts of Te or Se. The most troublesome impurities and defects causing reduction of lifetime have been shown to be C, Cu and Sb vacancies [23]. No information is available for carbon; however, experiments indicate that a small amount of carbon can drastically decrease the resistivity of AlSb.

2. EXPERIMENTAL

2.1 Bridgman Growth of AlSb

For the study of AlSb growth by the Bridgman method a vertically oriented two-zone type furnace was used. The hot and cold zones of the tube furnace were lined with Inconel heat pipes (6 inches long, 2.25 inch diameter) using sodium as

heat transfer fluid. The gap between the heat pipes, 2 inches, was filled with ceramic insulation. Temperature control and monitoring was provided by two temperature controllers and three K-type thermocouples located in the cold, hot and adiabatic zones respectively. For casting and growth of AlSb, Al and Sb (Alfa Products) of 6N grade (with respect to metal impurities) was used as starting material; high density alumina, graphite crucibles and GE-124 type quartz tubing was used. Before synthesis and growth, the aluminum was chemically etched in a solution of HF:H₂O₂ (1:2) for about two minutes and then in HNO₃:HCl (1:1) for about 30 s [12]. The antimony was purified by sublimation in quartz ampoules under dynamic vacuum. The alumina or graphite crucibles containing a mixture of Al and Sb in the desired proportions were located in graphite coated quartz ampoules and vacuum sealed. The charge was slowly heated to 1 090 °C, held at that temperature for 12 hours for homogenization and then solidified, passing through the temperature gradient with a constant speed. In different growth experiments, the temperature gradient of the adiabatic zone was varied from 5 °C/cm to 55 °C/cm, and the growth rate from 0.8 cm/hr to 1 cm/day, respectively, depending on the composition of the AlSb.

2.2 Czochralski Apparatus.

For Czochralski growth of AlSb an ADL (Arthur D. Little, Inc.) Model-LP apparatus was used, consisting of the growth chamber, two pulling mechanisms and a vacuum system (fig.3). The growth chamber was modified by adding an RF heating coil, temperature liner and crucible holder. The temperature of the crucible was calibrated versus RF current, monitored by a digital meter and controlled by the pick-up coil loop and differential amplifier. Growth was performed under an argon pressure of 40 PSI. Prior to growth, the crucible was annealed for 12 hrs at 1100 °C under vacuum. The starting Al and Sb components were prepared by the manner described for Bridgman growth. The typical weight of the AlSb used in the Czochralski system was in the range of 180-250 g.

2.3 THM Growth

The traveling heated method (THM) growth apparatus consists of a single vertical furnace with a narrow (spike type) temperature profile. The maximum peak temperature used in THM was 850 °C with a temperature gradient on both sides of the peak at about 75 °C/cm. Graphite coated quartz ampoules, filled at the bottom with a 10 mm long pure Sb ingot and at the top with a 66 mm long Czochralski grown AlSb ingot were used. The growth rate was about 1 to 5 mm/day.

3. RESULTS AND DISCUSSION

2.1 Bridgman Growth from Congruent Melt

Bridgman growth from a congruent melt of AlSb heavily wet both the alumina and graphite crucibles. Moreover, during growth and cool-down to room temperature, the volume change of the AlSb crystal often caused the alumina and graphite crucibles to crash. Near-infrared transmission microscopy scanning performed on double-side polished samples showed a poly-type structure with macro-grains and many cracks inclusions (fig. 4). Electrical measurements performed at room and nitrogen temperatures show p-type conductivity in both cases. Resistivity, carrier concentration and mobility were in the ranges 0.1 to 10 cm^{-3} , $(1 \text{ to } 8) \times 10^{17} \text{ cm}^{-3}$ and 79 to 180 cm^2/Vs , respectively. Optical measurements, performed in the wavelength range from 0.7 to 16 μm (fig. 5), showed a sharp cut-off near 1.6 eV related to the band-to-band transition, a plateau in the energy range 0.9 to 1.6 eV, a small absorption feature with a maximum near 0.75 eV and monotonically increasing absorption of free carriers below 0.5 eV. The feature near 0.75 eV, interpreted as the interband photon-carrier interaction between the spin-orbit split band and heavy hole band, disappeared when the material was n-type. In the intermediate wavelength range (0.9 to 1.6 eV) the lowest absorption coefficient for Bridgman grown material was about 10 cm^{-1} .

3.2 Bridgman Growth from Off-Stoichiometric Melt

As the AlSb melt was enriched with excess antimony, the solidus temperature was lowered, significantly reducing the tendency for wetting and crucible and/or material crashing. For example, using 70 mol % Sb and 30 mol % Al, the growth temperature was lowered to about 980 °C. As shown by Sherohman [21], the Sb vacancies should decrease about six times; however, the carrier concentration, determined from Hall and resistivity measurements, was in the range of $5.7 \times 10^{16} \text{ cm}^{-3}$, three to four times lower-than data obtained for samples grown from a congruent melt. Microscopic observations of the samples grown from off-stoichiometric melt clearly reveal grain and sub-grain boundaries, but no inclusions or macro-precipitates (fig. 6). The main disadvantages of off-stoichiometric melt growth, however, were a very slow growth rate ($\sim 1 \text{ cm/day}$) and difficulty obtaining large single crystals.

3.3 Czochralski Growth

AlSb crystals grown by the Czochralski method revealed several significant advantages over Bridgman grown material. The ingot was virtually always free of cracks, inclusions and large precipitates. The growth rate was more controllable and the seeding more effective in obtaining large single grains. Optical scanning showed mostly grain boundaries, twins and some single, small precipitates (fig. 7). Electrical and optical characteristics of the Czochralski-grown material, however, were strongly related to the growth time and the volume of the charge. During growth the composition of the melt changes due to Sb losses; this affects

the optical and electrical properties of the grown material. For example, the absorption coefficient, α , increases with the growth time (fig. 8). Corresponding electrical measurements show an order of magnitude change in carrier concentration and mobility. To overcome this problem, a larger volume of charge (>250g) and several percent excess Sb was used to compensate for losses; this, however, brought new complications: the growth rate versus time was no longer constant and the cost of the experiment increased. An experiment with liquid encapsulation showed negative results. B_2O_3 as well as all chlorides and fluorides react with AlSb and because of excessive evaporation completely covered the window, decreasing visibility to zero. Experimental results show that contamination can come from contact with the crucible material but also from the vapor phase; for example, SIMS analyses showed that the carbon concentration can be as large as $3 \times 10^{17} \text{ cm}^{-3}$ if a graphite susceptor or crucible is used. Experimentation with different crucible materials (e.g. alumina, pyrolytic graphite, boron nitrate) and different susceptor materials (e.g. graphite, titanium, Inconel and iron) indicated best results with the alumina crucible and graphite susceptor. The maximum argon over-pressure used in this system was 45 PSI. Currently being designed is a system which will permit operation at pressures of a few thousand PSI.

3.4 THM Growth

THM, an alternative method for growth of high quality AlSb, is based on forcing a narrow molten zone of solution through a solid ingot. During the slow movement of the liquid zone through the ingot, dissolution occurs at the top and recrystallizing at the bottom. The main advantages of this growth process are significant improvements in defect density, impurity concentration and compositional homogeneity. AlSb growth experiments by THM reveal that the concentration of uncompensated vacancies can be as low as $7.6 \times 10^{15} \text{ cm}^{-3}$ and hole mobility as high as $342 \text{ cm}^2/\text{Vs}$ at 300 K. Evidence for the effectiveness of THM is provided in fig.9. For growth with the same geometry and bias, photoconductivity of THM grown sample is an order of magnitude larger than that of the best sample grown by the Czochralski method. The main disadvantages of the THM technique, however, are extremely slow growth rate (1 to 5 mm/day) and limited size of crystals (the ingot usually contained many randomly oriented grains). Additional disadvantages of this growth method were the requirement for good quality crucibles and pre-grown solid AlSb seed material.

The low resistivity of AlSb can be attributed to the presence of very shallow acceptors which, as shown by low temperature analyses; activation energy of these is in the range of 0.026 eV. The nature of these acceptors is still unknown, though there is evidence that they may be antisite type defects or carbon impurities. In this context, a doping study has been carried out using initially Se and later Te and S as dopant. Se-doped crystals were grown by the Czochralski technique using Sb-rich melt. A series of crystals grown with different

concentrations of Se added to the melt had differing results. For example, the addition of 10^{18} cm⁻³ Se produces an n-type material with the room temperature free electron concentration as high as 3×10^{17} cm⁻³. Se-doped crystals have exhibited a free carrier freeze-out that is evident in the temperature dependence of the resistivity. It has been found that illumination of crystals at low temperature result in a reduction of resistivity which persists after the light was removed. A similar effect was observed in spectral absorption measurements.

4. REFERENCES

1. L.D. Lande, M. Cardona and F.M. Pollak, Phys. Rev. 131 (1970), 1436.
2. R.K. Willardson, A.C. Beer and A.E. Middleton, J. Electrochem. Soc. 101 (1954) 354.
3. J.M. Yee, S.P. Swierkowski and J.W. Sherohman, IEEE Trans. Nucl. Sci. 24 (1977) 1962.
4. R.J. Stirn and W.M. Becker, J. Appl. Phys. 37 (1966) 3616.
5. Y. Aguev and A.R. Mikhailov, Soviet. Phys. Semicond. 6 (1973) 1263.
6. H. Welker, Z. Naturforsch. 7a (1952) 744.
7. H. Welker, Z. Naturforsch. 8a (1953) 248.
8. R. Linneback and K.W. Benz, J. Crystal Growth 53 (1981) 579.
9. W.P. Allerd, B. Pavis and M. Gensen, J. Electrochem. Soc. 105 (1958) .
10. W.P. Allerd, W.L. Mefferd, R.K. Willardson, J. Electrochem. Soc. 107 (1960) 117.
11. C.T. Lin, E. Schonherr and H. Bonder, J. Crystal Growth 104 (1960) 653.
12. C.T. Lin, E. Schonherr, H. Bonder and C. Busch, J. Crystal Growth 94 (1959) 955.
13. M. Leroux, A. Tromson-Carli, et al., J. Crystal Growth 48 (1980) 367.
14. E.A. Owen and G.D. Preston, Proc. Phys. Soc. (London) 36 (1924) 341.
15. R.K. Willardson, A.C. Beer and A.E. Middleton, J. Electrochem. Soc. 101 (1954), 354.
16. R.F. Blunt, M.P.R. Frederikse, J.H. Becker and W.R. Hosler, Phys. Rev. 96 (1954), 578.
17. V.M. Glazov and D.A. Petrov, Izv. Akad. Nauk SSSR Otd. Tekn. Nauk 25. (1958).
18. M. Hansen, Constitution of Binary Alloys, McGraw-Hill Book Co., New York (1958).
19. J.A. Van Vechten and J.C. Phillips, Phys. Rev B2 (1970) 2160.
20. D.J. Miller and D. Heneman, Phys. Rev. B 3 (1971) 2918.
21. J.W. Sherohman, J. Electrochem. Soc. (1978).
22. A. Hercy, R.R. Haberecht and A.E. Middleton, J. Electrochem. Soc. 105 (1958), 533.
23. J.W. Mayer, Semiconductor Detectors, G. Bertolini and A. Coche, Eds. American Elsevier Publishing Company, Inc., New York (1968).
24. P.M. Mooney, J. Appl. Phys. 67 (1990).

25 P. Becla, A.F. Witt, J. Lagowski and W. Walukiewicz, Appl. Phys. Lett.
67,(3) 395 (1995)

DISCLAIMER

This report was prepared as an account of work sponsored by an agency of the United States Government. Neither the United States Government nor any agency thereof, nor any of their employees, makes any warranty, express or implied, or assumes any legal liability or responsibility for the accuracy, completeness, or usefulness of any information, apparatus, product, or process disclosed, or represents that its use would not infringe privately owned rights. Reference herein to any specific commercial product, process, or service by trade name, trademark, manufacturer, or otherwise does not necessarily constitute or imply its endorsement, recommendation, or favoring by the United States Government or any agency thereof. The views and opinions of authors expressed herein do not necessarily state or reflect those of the United States Government or any agency thereof.

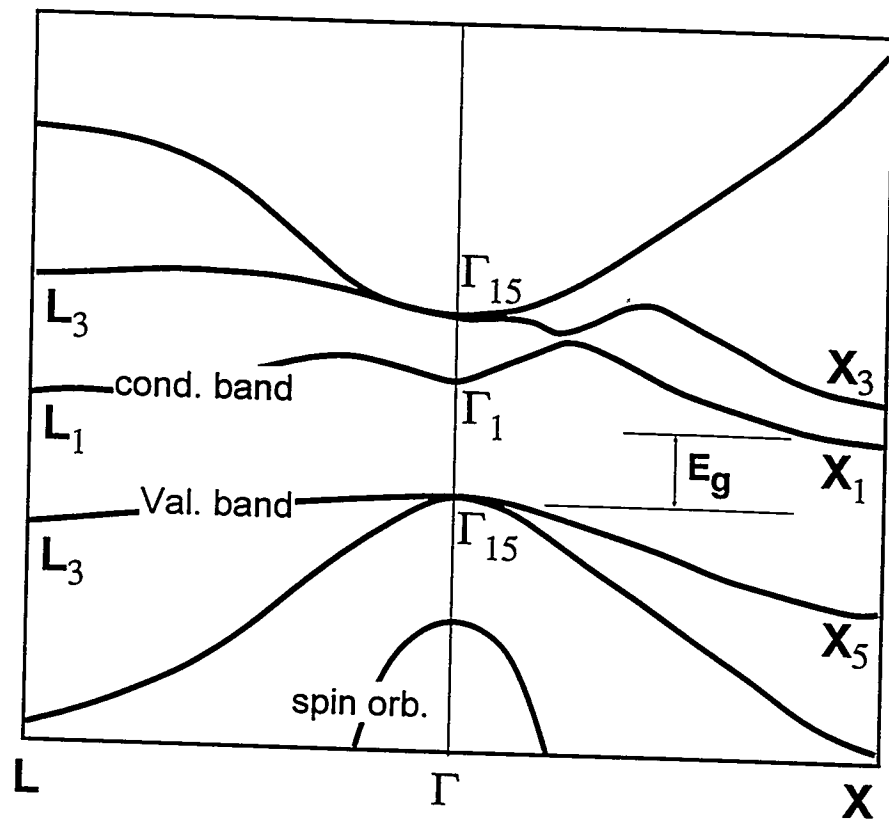


Fig. 1 Band structure of AlSb [3].

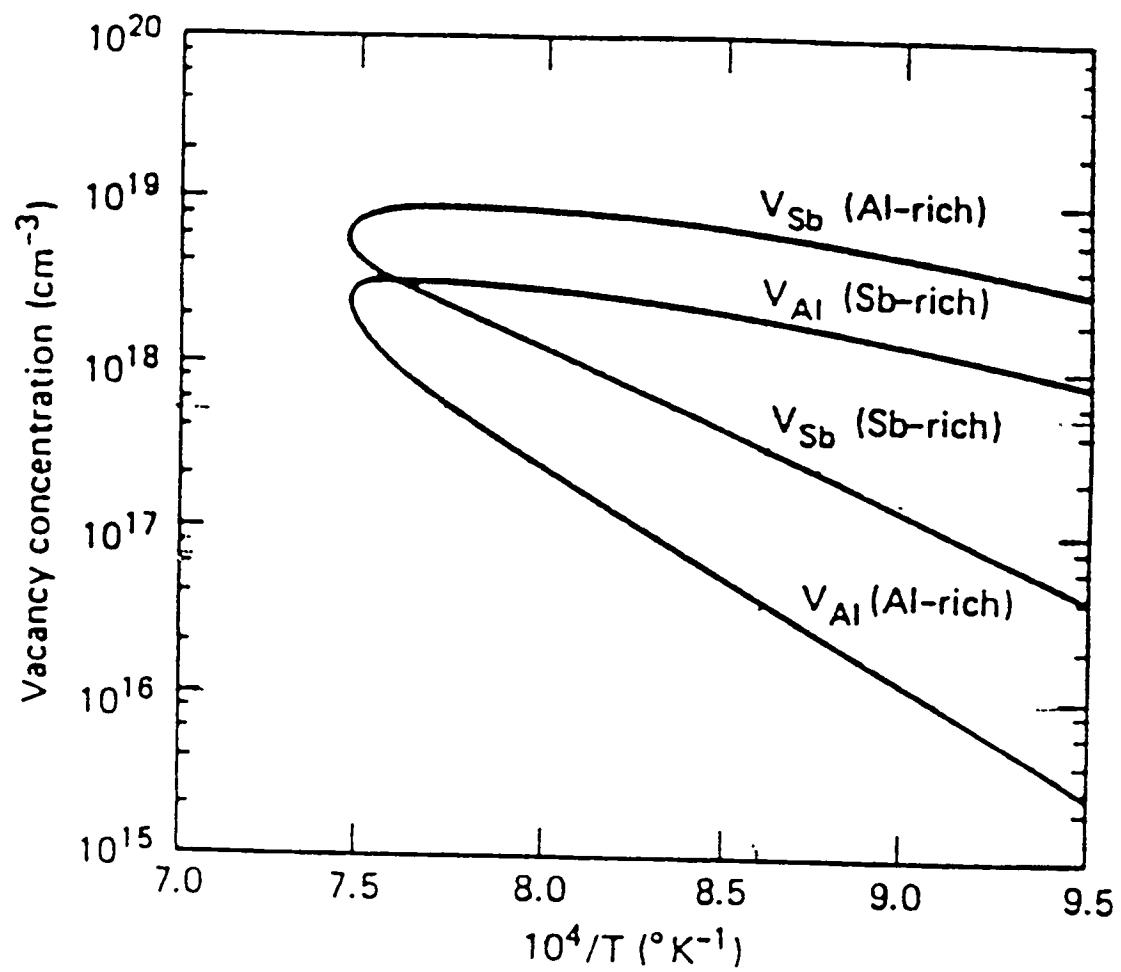


Fig.2 Al and Sb vacancy concentration versus temperature of AlSb solid solution [21].

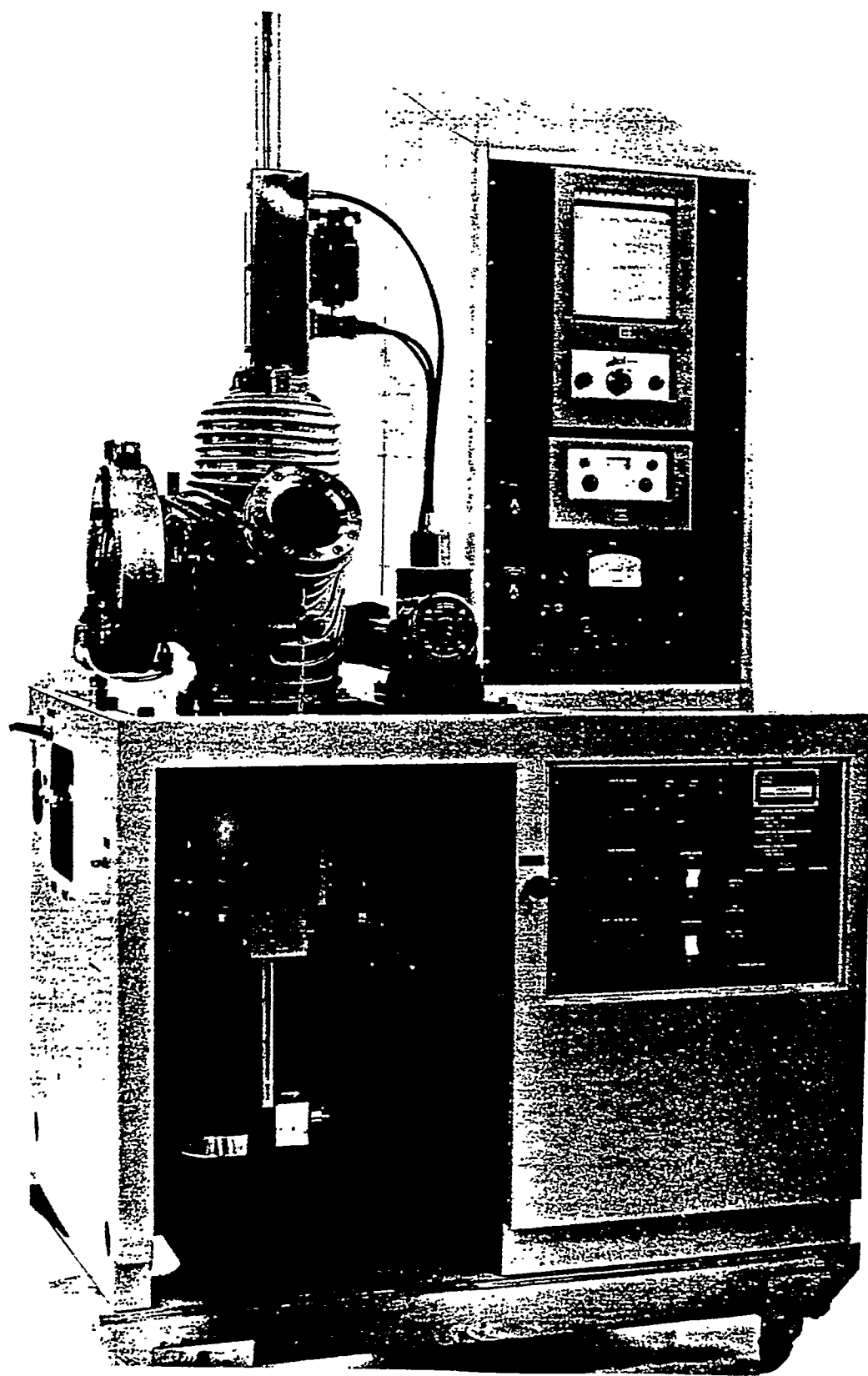


Fig.3 Top-seed Czochralski growth apparatus.



Fig 4 Near infrared scanning spectroscopy image of AlSb grown by the vertical Bridgeman method using stoichiometric melt

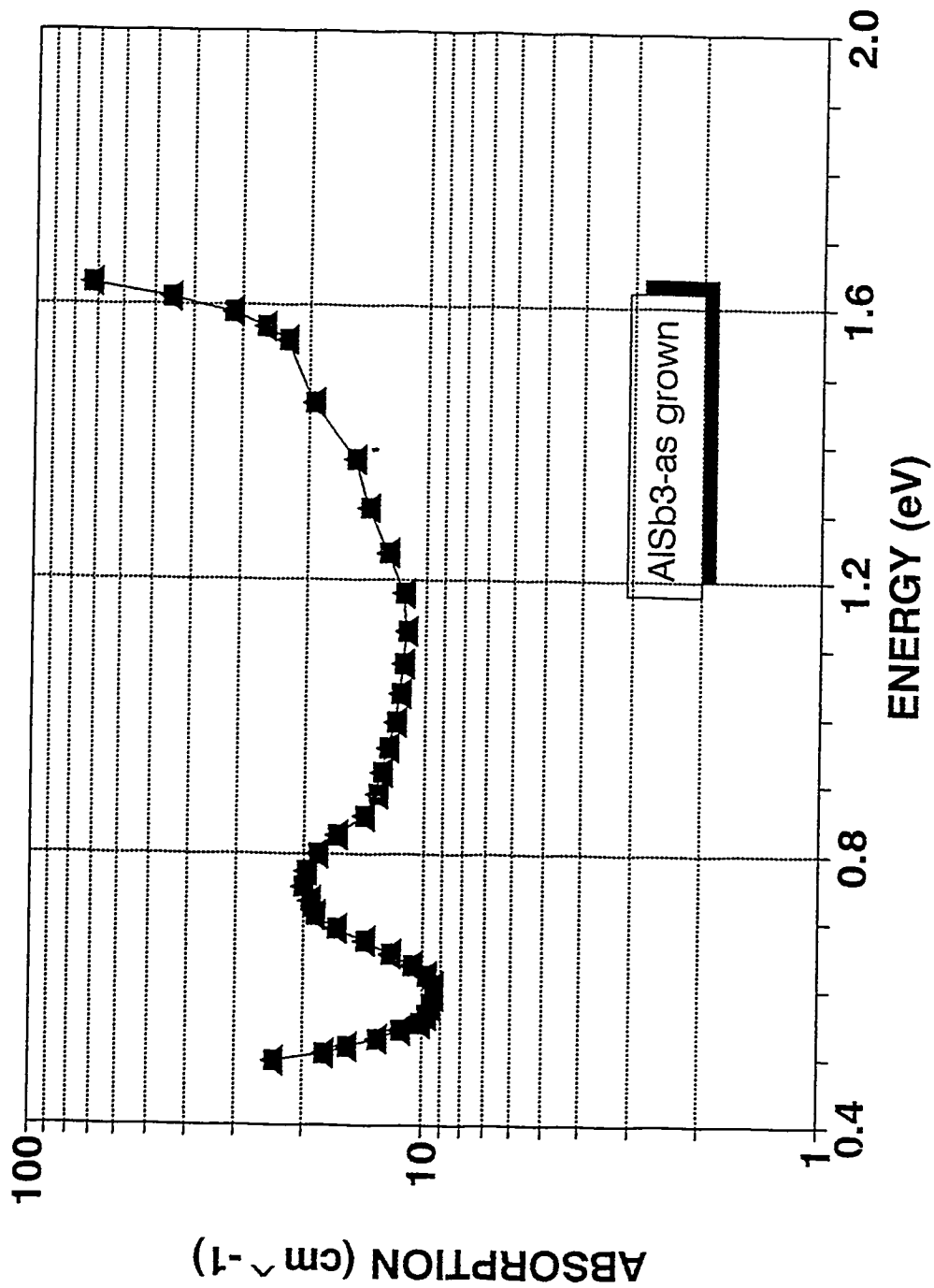


Fig. 5 Spectral absorption characteristics of AlSb crystals grown by the vertical Bridgman techniques.

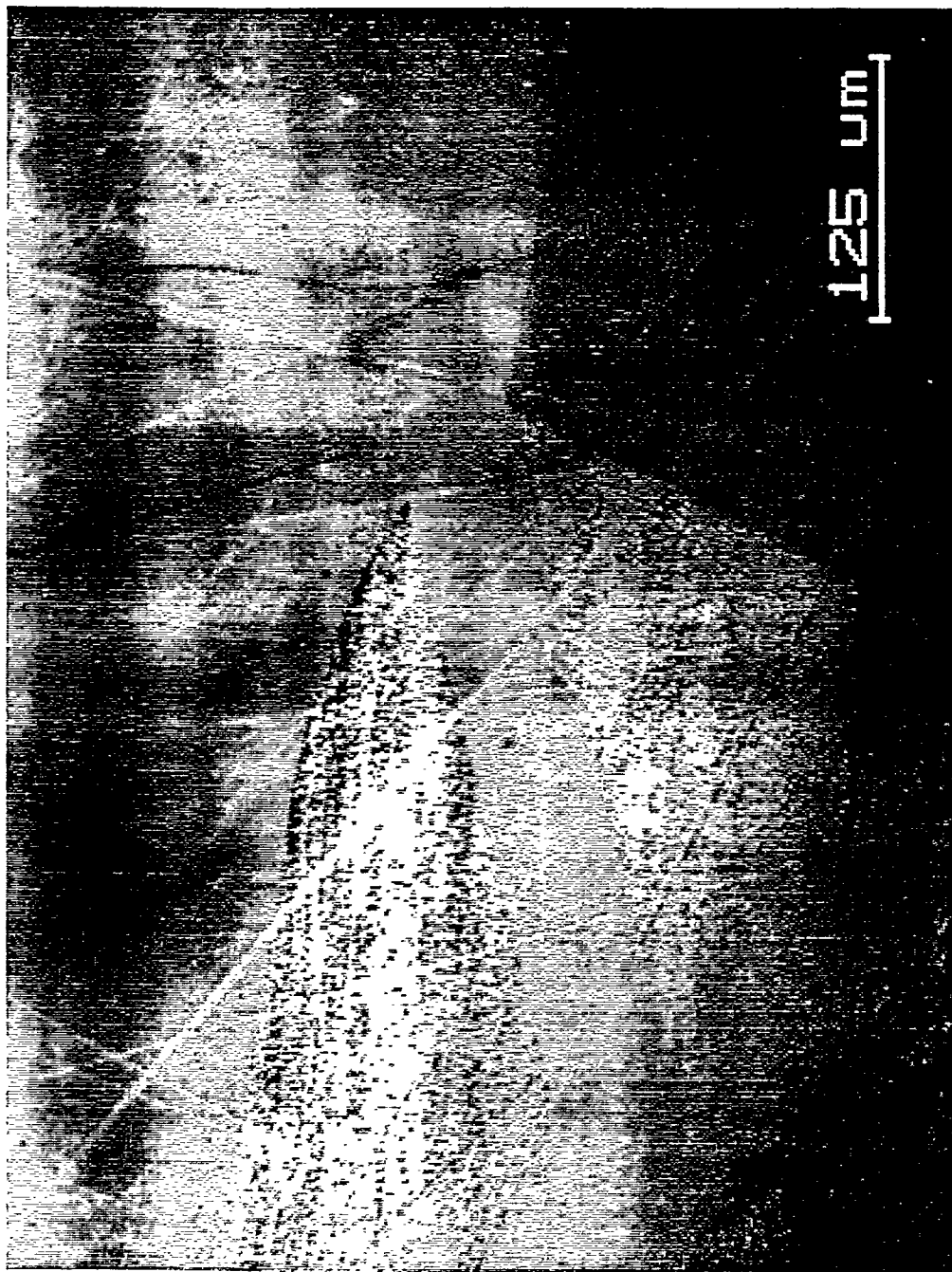


Fig.6 Near infrared scanning spectroscopy image of AlSb grown by the vertical Bridgeman method using off-stoichiometric melt.



Fig.7 Near infrared scanning spectroscopy image of AlSb grown by the Czochralski techniques.

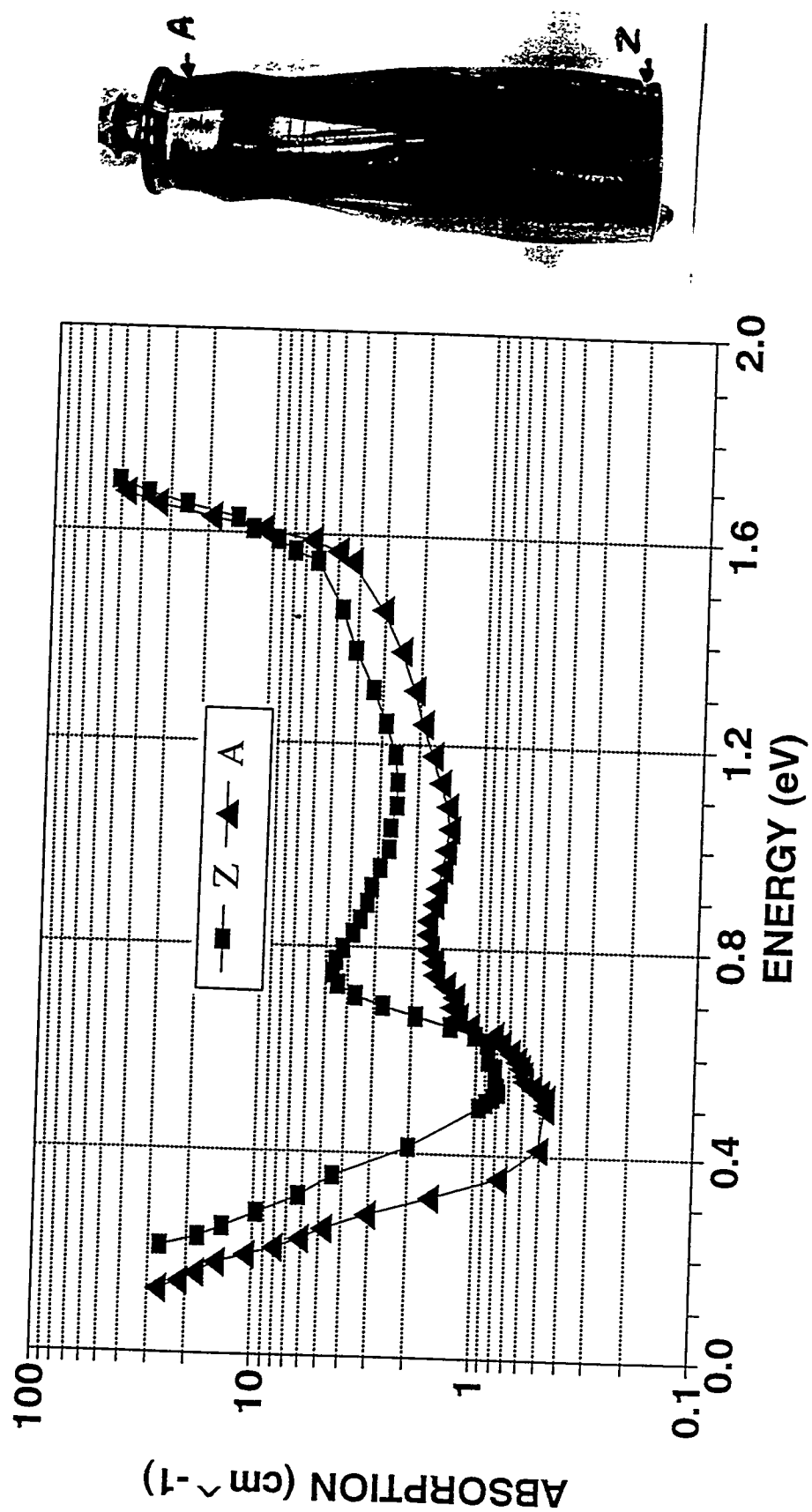


Fig.8 Spectral absorption characteristics of the AlSb crystals grown by the Czochralski techniques.

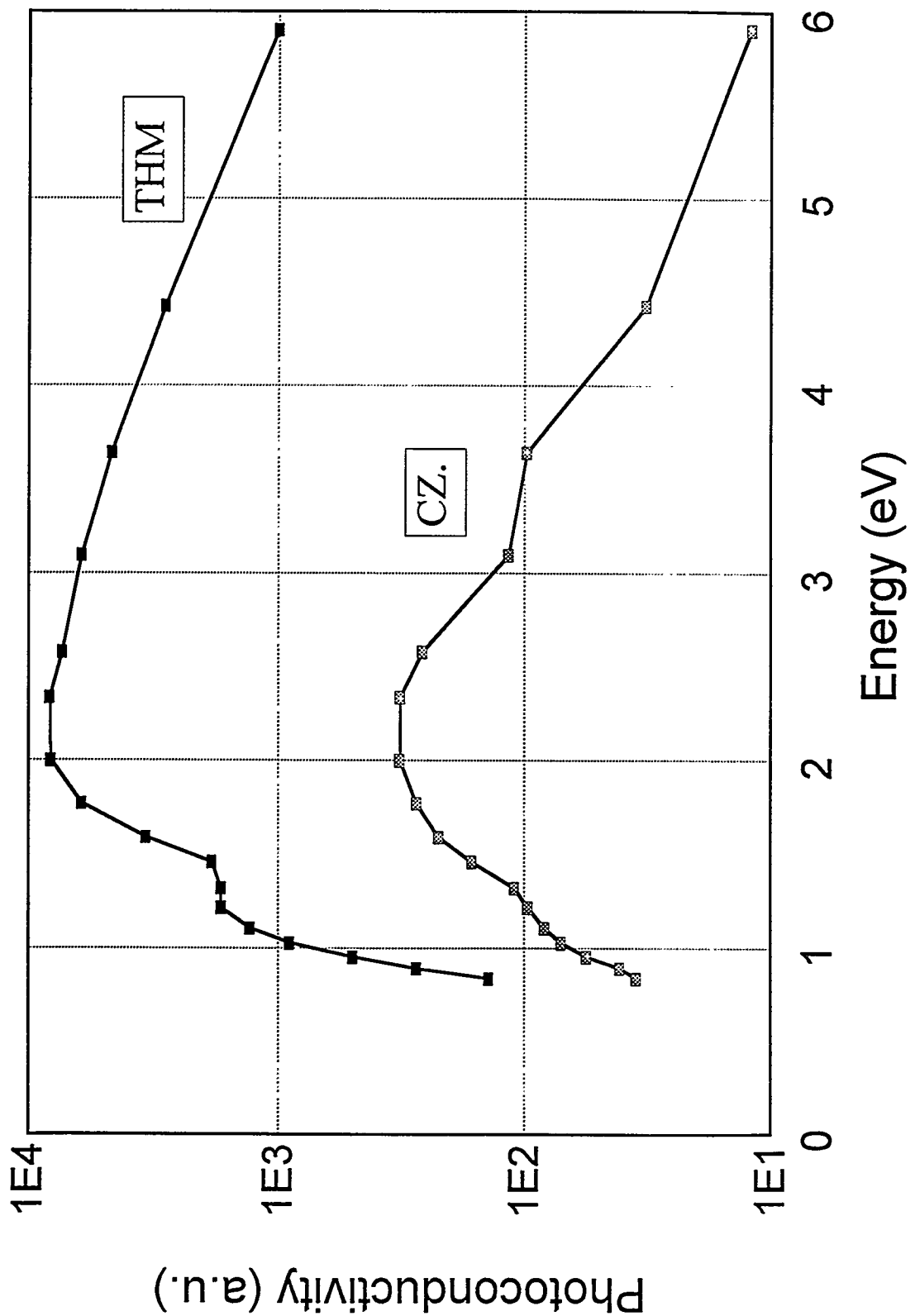


Fig.9 Spectral photoconductivity characteristics of AlSb crystals grown by THM and Czochralski techniques.